PRESSURE TRANSIENT ANALYSIS OF CO_2 AND ENRICHED GAS INJECTION AND PRODUCTION WELLS

Don J. MacAllister
ARCO Exploration and Technology Company

ABSTRACT

A theoretical basis for pressure transient analysis of gas wells with emphasis on the real gas pseudo pressure approach is outlined. An analysis procedure is developed to analyze wells either injecting or producing predominatly CO_2 or enriched gas. This procedure is used to calculate flow capacities and skin factors from pressure transient tests in injection and production wells from two CO_2 projects. A computer program is documented which aids in the analysis of gas wells with the real gas pseudo pressure. Finally, example calculations are shown for a CO_2 well, an enriched gas well, and an enriched gas well contaminated with CO_2 / H_2S.

INTRODUCTION

Pressure transient analysis is one of the most widely used methods in reservoir engineering to obtain in-situ reservoir data. A variety of transient testing techniques have been developed including pressure buildup, pressure drawdown, injectivity, pressure falloff, and interference testing[1,2]. Reservoir data calculated from these techniques includes wellbore volume, wellbore damage or stimulation, reservoir pressure, flow capacity (permeability), reserves, fracturing, reservoir discontinuities, fluid discontinuities and swept volume.

Pressure transient analysis was developed for liquid filled reservoirs with a small total compressibility. The solution of the diffusivity equation for a liquid filled reservoir results in a derivitive of pressure with respect to time. This is the basis of the pressure vs time plot used to determine reservoir properties. The classical liquid filled reservoir analysis has been extended to gas wells by three different approaches. The first is by analogy to the classical liquid filled reservoir analysis. This is possible through the use of average gas viscosity (μ_g), gas z factor (z), and gas compressibility (C_g) at the reservoir temperature, T, and average reservoir pressure, p. These assumptions are good in most gas reservoirs below 2000 PSI as long as pressure gradients in the reservoir are small, since for most natural gas wells, $\mu_g \cdot z$ at these conditions is approximately constant, figure 1[2]. Above this pressure, $(\mu_g \cdot z) / p$ is approximately constant. This gives rise to the second approach, where p^2 instead of p is analyzed as a fuction of time. The p^2 vs time relationship is used because the solution of the diffusivity equation for a gas filled reservoir yields a derivitive of p^2 with respect to time. In many cases the assumptions of constant μ_g, z, C_g, and small pressure gradients are not met and both the p and p^2 methods are invalid. As a result, a third approach was formulated which accounts for variations in μ_g and z as a function of p and allows large pressure gradients making the approach much more accurate. This is achieved through the use of a real gas pseudo-pressure function, m(p), which is a function of p, μ_g, and z and which matches figure 1 exactly. With this function, the solution of the diffusivity equation for a gas filled reservoir results in a derivitive of m(p) with respect to time; therefore m(p) instead of p or p^2 is analyzed as a fuction of time.

The m(p) function has been applied extensively in natural gas reservoirs and many sources of natural gas m(p) data are available[2]. The use of the real gas pseudo-pressure is not limited to gas wells, but can be applied to any flowing fluids as long as effective viscosities and compressibilities can be calculated. The wide application of miscible gas processes in the field has given rise to another set of pressure transient tests which can be analyzed with the real gas pseudo-pressure; those injecting or producing predominantly miscible gas, either CO_2 or enriched natural gas. This report documents application of the m(p) approach to such wells.

THEORETICAL BASIS

Pressure transient analysis is based on the radial diffusivity equation. This equation may be solved for slightly compressible liquids (the classical pressure transient analysis) yielding the derivitive of p with respect to time, for an ideal gas yielding the derivitive of p^2 with respect to time, and with the real gas pseudo-pressure yielding the derivitive of m(p) with respect to time.

Mathematical Basis of Pressure Transient Analysis

Assuming radial flow, constant compressibility, isothermal conditions, constant average permeability, constant fluid viscosity, and small pressure gradients, the well known diffusivity equation can be derived[2]:

$$\frac{\partial^2 p}{\partial r^2} + \frac{1}{r}\frac{\partial p}{\partial r} = \frac{\o\, c_t\, \mu}{k}\;\frac{\partial p}{\partial t} \quad \cdots\cdots\cdots\cdots\cdots \quad (1)$$

Equation 1 contains the derivitive of p with respect to time. This equation can be solved using an exponential integral which may be reasonably approximated by:

$$p_{wf} = p_i - \frac{162.6\; q\; B_g\; \mu}{k\; h}\left[\log \frac{k\,t}{\o\;\mu\; c\; r_w^2} - 3.23\right] \quad \cdots\cdots \quad (2)$$

A plot of p vs t on log paper yields a straight line with a slope proportional to the flow capacity (kh). This equation applies for liquid filled reservoirs and natural gas reservoirs below 2000 PSI (see introduction). For natural gas reservoirs above 2000 PSI, the real gas law is used and the diffusivity equation is:

$$\frac{\partial^2 p^2}{\partial r^2} + \frac{1}{r}\frac{\partial p^2}{\partial r} = \frac{\phi c_t \mu}{k}\frac{\partial p^2}{\partial t} \cdots\cdots\cdots \quad (3)$$

This equation contains the derivitive of p^2 with respect to time. Since this equation is nonlinear it cannot be solved directly, however the following approximation was derived by analogy after interpreting finite difference solutions to equation 3[2]:

$$p_{wf}^2 = p_i^2 - \frac{1637\, q \mu z T}{k\, h}\left[\log \frac{k t}{\phi \mu c r_w^2} - 3.23\right] \cdots\cdots \quad (4)$$

A plot of p^2 vs t on log paper will yield flow capacity (kh). This equation applies to natural gas reservoirs above 2000 PSI.

Real Gas Pseudo-Pressure

The real gas pseudo-pressure function, m(P), was first published by Al-Hussainy, Ramey, and Crawford[5], and is defined as:

$$m(p) = \int_{p_b}^{p} \frac{p}{\mu(p)\; z(p)}\, dp \cdots\cdots\cdots \quad (5)$$

Use of equation 5 avoids the assumptions of constant μ_g, z, C_g, and small pressure gradients necessary in the previous two approaches. The variable p_b is an arbitrary base pressure which is usually choosen as 14.7 PSI. In this form, the μ_g and z vary with pressure. Al-Hussainy, et. al.[5] inserted this function into the gas diffusivity equation yielding:

$$\frac{\partial^2 m(p)}{\partial r^2} + \frac{1}{r}\frac{\partial m(p)}{\partial r} = \frac{\phi c_t \mu}{k}\frac{\partial m(p)}{\partial t} \cdots\cdots\cdots \quad (6)$$

As before this equation is nonlinear and cannot be solved directly, however Al-Hussainy, et. al.[5] solved equation 6 by analogy after interpreting finite difference results:

$$m(p_{wf}) = m(p_i) - \frac{1637\ q\ T}{k\ h} \log\left[\frac{k}{\phi\ \mu\ c\ r_w^2}\right] - 3.23 + 0.87\ S \qquad (7)$$

Equation 7 applies prior to the onset of boundary effects (well drainage radius). A semilog graph of $m(p_{wf})$ vs time should yield a straight line. The slope, m, of the straight line is related to the flow capacity, $k_g \bullet h$, as follows:

$$m = \frac{1637\ q\ T}{k_g\ h} \cdots\cdots\cdots\cdots \qquad (8)$$

or:

$$k_g h = k\, k_{rg} h = \frac{1637\ q\ T}{m} \cdots\cdots\cdots\cdots \qquad (9)$$

Note that the flow capacity is proportional to the effective gas permeability not the total permeability if gas dominates the flowing fluids. This implies that the the flow capacity is variable and will change with changes in the gas saturation since gas relative permeability is a function of gas saturation. If significant fractions of oil and/or water are also flowing, the flow capacity is proportional to the effective total fluid mobility. This quantity is not easily approximated and is usually determined by simulation.

Equation 7 can be rearranged to determine the skin factor, s:

$$S = 1.151 \frac{m(p_i) - m(p_{1hr})}{\dfrac{1637\ q\ T}{k_g\ h}} - \log \frac{k}{\phi\ \mu\ c\ r_w^2} + 3.23 \cdot \cdot \qquad (10)$$

ANALYSIS PROCEDURE

The pressure response in traditional pressure transient analysis is characterized by three regions on a semilog plot of p vs time. The first is wellbore storage at early times followed by two straight line regions; the fluid filled region and the well drainage region at late times[1-2].

When a well is shut-in, fluid flows back into the wellbore until it is filled. The storage capacity of the wellbore has nothing to do with reservoir properties and these effects must be identified so that the proper data is analyzed. An analysis of wellbore storage shows that :

$$C = \frac{q\,B\,\Delta t}{24\,\Delta p} \quad \cdots\cdots\cdots\cdots \quad (11)$$

A log log plot of Δt vs Δp will yield a straight line of unit slope as long as this equation holds. In the analysis outlined here log log plots are made to identify the data dominated by wellbore storage.

For an EOR displacement such as steam or miscible gas injection, the pressure response should be characterized by wellbore storage and three straight lines on a semilog plot of m(p) vs time corresponding to the miscible gas swept region, the miscible gas unswept region, and the well drainage boundary[3-4]. In practice the second and third lines are usually not separate, and only two straight lines exist. In addition if the CO_2 front is not sharp (almost always the case), there is a smooth transision between the two straight lines as opposed to a sharp transition for a sharp mobility front such as a steam front. Flow capacity and skin are determined from the slope of the straight line portion of the m(p) vs time curve lying between the storage dominated portion and the final straight line.

The pressure transient tests analyzed in this report were done with the aid of a FORTRAN program listed in Appendix A. Inputs required are flow rates and times prior to shut-in, initial pressure, and an array of shut-in pressure vs time. In addition an array of pressure from 14.7 PSI (or some other convienent reference pressure below the pressures encountered in the test) to a pressure above the maximum pressure recorded in the field test is needed to calculate the real gas pseudo-pressure. For each pressure in this array a gas viscosity and compressibility (z factor) is also read in. The program then generates arrays of time, horner function, summation function, pressure, m(p), and $\Delta m(p)$.

In the following two sections the procedure for determining gas viscosity and compressibility for calculation of the real gas pseudo-pressure function is outlined. The first section is for a well injecting or producing predominatly CO_2 and the second section is for a well injecting or producing predominatly enriched gas.

CO_2 Well

If the well is injecting or producing predominatly CO_2, calculation of compressibility and viscosity is straightforward. CO_2 compressibility at reservoir temperature and several pressures can be determined from data contained in table 4[6]. CO_2 viscosity at reservoir temperature and several pressures can be determined from figure 2[7] through the use of reduced viscosity, reduced pressure, and reduced temperature defined as follows:

$$\mu_r = \mu / \mu_c(CO_2) = \mu / 3335 \cdot 10^{-5}\,\text{cp} \quad \cdots\cdots \quad (12)$$

$$P_r = p / P_c(CO_2) = p / 72.8\,\text{atm} \quad \cdots\cdots \quad (13)$$

$$T_r = \frac{(T^\circ F + 460) / 1.8\ ^\circ K / ^\circ F}{Tc\ (CO_2)} = \frac{(T^\circ F + 460) / 1.8\ ^\circ K / ^\circ F}{304.2^\circ K} \quad \cdots\cdots \quad (14)$$

Enriched Gas Well

If the well is injecting or producing predominatly enriched gas, gas compressibility and viscosity at reservoir temperature and several pressures can still be determined, but the procedure is more involved. First a critical pressure, Pc and temperature, Tc, are determined for the gas mixture using the following mixing rules[8,9]:

$$J = 1/3 \sum y_j \cdot (Tc/Pc)_i + (2/3) \cdot \left[\sum y_j \cdot (Tc/Pc)_i^{0.5} \right]^2 \quad \cdots\cdots \quad (15)$$

$$K = \sum y_j \cdot (Tc/Pc)_i^{0.5} \quad \cdots\cdots \quad (16)$$

$$Tc = K^2 / J \quad \cdots\cdots \quad (17)$$

$$Pc = Tc / J \quad \cdots\cdots \quad (18)$$

Enriched gas compressibility at reservoir temperature and several pressures can then be determined from reduced property charts using equations 13 and 14 and figures 3a and 3b[10]. Gas viscosity is determined from the Dean and Stiel equations[11]:

$$(\mu - \mu^\circ)\,\xi = 1.08 \left[\exp 1.439\,\rho r - \exp(-1.11\,\rho r^{1.858}) \right] \quad \cdots\cdots \quad (19)$$

$$\mu^\circ \xi = 3.40\, Tr^{8/9} \qquad Tr \leq 1.5$$

$$= 16.68\,(0.1338\, Tr - 0.0932)^{5/9} \qquad Tr > 1.5 \quad \cdots\cdots \quad (20)$$

$$\xi = Tc^{1/6} / M^{1/2}\, Pc^{2/3} \quad \cdots\cdots \quad (21)$$

$$M = \sum M_j \quad \cdots\cdots \quad (22)$$

$$\rho r = Vc / V \quad \cdots\cdots \quad (23)$$

$$V = (ZRT)/P \quad \cdots \quad (24)$$

$$Vc = \sum y_j \, Vc_j \quad \cdots \quad (25)$$

If the enriched gas contains significant amounts of CO_2 and/or H_2S, Pc and Tc are further modified as described by Wichert and Aziz[12] before using the reduced property charts, figures 3 and 4:

$$\varepsilon = 120\,(A^{0.9} - A^{1.6}) + 15\,(B^{0.5} - B^4) \quad \cdots \quad (26)$$

where:

A = mole fraction ($CO_2 + H_2S$) and B = mole fraction H_2S

$$Tc' = Tc - \varepsilon \quad \cdots \quad (27)$$

$$Pc' = Pc\,Tc' / (Tc + B\,(1 - B)\,\varepsilon) \quad \cdots \quad (28)$$

APPLICATIONS

Injection well falloff tests and production well build-up tests were conducted in 1985 for wells injecting or producing predominatly CO_2 gas in a sandstone reservoir CO_2 flood (Resevoir 1). These tests were analyzed with the procedure outlined here, and for comparison, two injection well falloff tests conducted in 1983 were re-analyzed. In addition, injection well falloff tests conducted in 1982 in another sandstone reservoir CO_2 flood (Resevoir 2) are analyzed. The results are summarized in Table 1.

The methods described in the previous section were used to determine gas viscosity and z factor. Standard pressure transient techniques were employed in the analysis of the plots. Wellbore storage was determined using the unit slope method (equation 11) and several wells were determined to be fractured using the half slope method on storage plots[1-2]. Flow capacity and skin were determined using equations 9 and 10.

Reservoir 1

The pressure transient analysis was done with the parameters outlined in Tables 2 and 3. The pressure transient data were uninterpretable for injection well #18, Figure 4, because the response is dominated by wellbore storage; and for injection wells #64 and #74 (1985), figures 13 and 14, due to fracturing. Although injection well #29 (analyzed both in 1983 and 1985), figures 5 and 7, has a half slope region, it occurs in the the boundary dominated portion indicating that the half slope is a boundary effect and the test results are valid. The results for production well #409, figures 23 and 24, are questionable because the pressure began to fall after 30 hours shut-in time (table 17), indicating that a leak occurred.

The flow capacities (effective permeability to gas times thickness) varied from 1315 to 3137 md • feet for all injection wells except #74 (1983), table 1. Injection well #74 (1983) and the production wells have much lower flow capacities. This is consistant with low gas saturations during the initial injection in 1983 and shortly after gas breakthrough in the production wells. The flow capacity (the product of the reservoir thickness, absolute permeability, and relative permeability to gas, equation 9) will be lower since low gas saturation yields low gas relative permeability. If significant fractions of oil and/or water are also flowing, the flow capacity is proportional to the effective total fluid mobility. In this case, the flow capacity would still be low since the effective total fluid viscosity will be higher with water and/or oil flowing than the miscible gas viscosity.

All skin values are similar indicating stimulation by CO_2, except injection well #87 which has a very large skin. Wellbore damage in this well is evident by the very large pressure reduction of almost 500 PSI in the first 15 minutes of the falloff test, figures 17 and 18 and table 14.

Reservoir 2

The pressure transient analysis was done with the parameters outlined in Tables 2 and 3. The pressure transient data were uninterpretable for injection wells 62, figure 25, and 488, figure 28, because the response is dominated by fracturing. In injection well 487 the flow capacity (effective permeability to gas times thickness) is 140 md • feet which is consistant with a low gas saturation. The skin value is -1.9 indicating stimulation by CO_2.

Well by Well Interpretation

Reservoir 1 #18, Table 6 & Figure 4
The log-log plot yields a line of unit slope; indicating that the data is dominated by wellbore storage and therefore uninterpretable.

Reservoir 1 #29 (1985), Table 7 & Figures 5-6
The log-log plot indicates that the first few points are influenced by wellbore storage and the last dozen points have a half slope. These points are in the boundary region and donot therefore indicate fracturing. The proper points to analyze are those between these two regions. Flow capacity = 1949 md•ft; Skin = -1.8

Reservoir 1 #29 (1983), Table 8 & Figures 7-8
The log-log plot is similar to the previous (more recent) plot except the half slope region is larger implying that the CO_2 swept region was smaller in 1983 relative to 1985. Flow capacity = 1046 md•ft; Skin = -5.0

Reservoir 1 #39, Table 9 & Figures 9-10
The log-log plot indicates that wellbore storage is over quickly. The first straight line on the falloff plot is the correct one to choose. Flow capacity = 1315 md•ft; Skin = -0.2

Reservoir 1 #52, Table 10 & Figures 11-12
The log-log plot indicates that wellbore storage is over quickly. The first straight line on the falloff plot is the correct one to choose. Flow capacity = 1490 md•ft; Skin = -2.0

Reservoir 1 #64, Table 11 & Figure 13
The log-log plot indicates that wellbore storage dominates the first few points, while the remainder fall on a half slope line indicating that the well is fractured and uninterpretable.

Reservoir 1 #74 (1985), Table 12 & Figure 14
The log-log plot indicates that wellbore storage dominates the first few points, while the remainder fall on a half slope line indicating that the well is fractured and uninterpretable.

Reservoir 1 #74 (1983), Table 13 & Figures 15-16
The log-log plot indicates that wellbore storage is over quickly. The first straight line on the falloff plot is the correct one to choose. Apparently this well was fractured sometime between these two falloff tests. Flow capacity = 102 md•ft; Skin = -2.0

Reservoir 1 #87, Table 14 & Figures 17-18
The log-log plot indicates that wellbore storage is over after the first 5-7 pressure points. The falloff plot demonstrates a dramatic drop in pressure in a short period after the well is shut-in. This is indicative of a large positive skin factor. Again, the first straight line on the falloff plot is the correct one to choose. Flow capacity = 3137 md•ft; Skin = 47

Reservoir 1 #84, Table 15 & Figures 19-20
The log-log plot indicates that wellbore storage is over after the first 5-7 pressure points. The falloff plot shows a discontinuity in pressure at about 1 hour (50 on the horner plot). I assume that this is an artifact of the measuring system. If the gap between 0.5 and 1 hour (25 and 50 on the horner plot) is removed, the intermediate points lie on the indicated straight line. Flow capacity = 14.6 md•ft; Skin = -2.2

Reservoir 1 #95, Table 16 & Figures 21-22
The log-log plot indicates that wellbore storage is over after the first 5-7 pressure points. The falloff plot shows a pressure plateau from 0.1 hour to 3 hours (150 to 9 on the horner plot). Again, I assume that this is an artifact of the measuring system. The first straight line is choosen. Flow capacity = 94.0 md•ft; Skin = -2.3

Reservoir 1 #409, Table 17 & Figures 23-24
Both the log-log plot and falloff plot indicate that pressure builds up and then starts to fall at late times (~30 hours). This cannot happen in a pressure build-up test, and indicates that a leak occurred. Although this casts doubt on the validity of this test, the first straight line is choosen. Flow capacity = 28.4 md•ft; Skin = -2.2

Reservoir 2 #62, Table 18 & Figure 25
The log-log plot indicates that wellbore storage dominates the first 20 or so points, the drainage boundary isapparent in the last 10 points, and those points in between these two regions fall on a half slope line indicating that the well is fractured and uninterpretable.

Reservoir 2 #487, Table 19 & Figures 26-27
The log-log plot indicates that wellbore storage is over quickly. The first straight line on the falloff plot is the correct one to choose. Flow capacity = 140 md•ft; Skin = -1.9

Reservoir 2 #488, Table 20 & Figure 28
The log-log plot indicates that wellbore storage dominates the first couple of points, while the remainder fall on a half slope line indicating that the well is fractured and uninterpretable.

GAS WELL COMPUTER PROGRAM

A FORTRAN program was written to facilitate pressure transient analysis of gas wells using the real gas pseudo-pressure. First a set of pressures ranging from some low reference pressure (usually 14.7 PSI) to a pressure well above the reservoir pressure is input. CO_2 viscosity and z factor at reservoir temperature is also input for each pressure. Next a spline fit of $p / (\mu \cdot z)$ as a function of p is performed. The real gas pseudo-pressure, m(p), is twice the integral of this function. The m(p) function is calculated by integrating the polynomial expression derived in the spline fit. The program also calculates two time functions; the horner function and the summation function.

Spline Fit

In a spline fit, a set of n constants, C_i, i = 1 to n, is calculated for n pairs of data points. The expression for Y_{int} corresponding to an unknown X_{int} lying between two known data pairs (x_i and x_{i+1}) is given by[13]:

$$Y_{int} = C_1 (x_{i+1} - X_{int})^3 + C_2 (X_{int} - x_i)^3 + C_3 (X_{int} - x_i) + C_4 (x_{i+1} - X_{int}) \quad \cdots \quad (29)$$

where:

$C_1 = C_i / 6 h_j$ $\qquad$ $C_2 = C_{i+1} / 6 h_j$

$C_3 = Y_{i+1} / h_j - (C_{i+1} h_j) / 6$ $\qquad$ $C_4 = Y_i / h_j - (C_i h_j) / 6$

$h_j = x_{i+1} - x_i$

The integral of this function is:

$$\int Y_{int} = \frac{-C_1}{4} (x_{i+1} - X_{int})^4 + \frac{C_2}{4} (X_{int} - x_i)^4 + \frac{C_3}{2} (X_{int} - x_i)^2 - \frac{C_4}{2} (x_{i+1} - X_{int})^2 \quad \cdots \quad (30)$$

The m(p) function is twice the sum of integrals described by equation 30 for all x,y data pairs between x_1 and X_{int}. The program uses this algorithm to calculate arrays of pressure and m(p).

Summation Function

Arrays of time, horner function, and summation function are also calculated and tabulated. The horner function is well known in traditional pressure transient analysis[1] and is usually employed instead of time on the x axis. Classical pressure transient analysis also assumes that the well is produced or injected for a constant period prior to shut in. In many cases this is not true. The summation function corrects for multiple rates using the superposition principal to yield a time function equivalent to the horner function defined as[2]:

$$\text{summation function} = \sum_{j=1}^{n} \frac{q_j}{q_n} \log \left[\frac{tn + ts - t(j-1)}{tn + ts - tj} \right] \quad \cdots \quad (31)$$

Note that for a single injection rate of t hours duration; $q_j = q_n$; $t_n = t_j = t$; and $t_{j-1} = 0$. In this case the summation function reduces to :

$$\log \left(\frac{t+t_s}{t_s} \right) \quad \cdots \quad (32)$$

This is the definition of the horner function.

EXAMPLES

Three example calculations are presented below to illustrate viscosity and compressibility determinations: a CO_2 well, an enriched gas well, and an enriched gas well contaminated with CO_2 / H_2S.

Example 1: CO_2 Well

Reservoir Temperature: 235°F
Reservoir Pressure: 4000 PSI
CO_2 Tc : 304.2°K
CO_2 Pc : 72.8 atm

First reduced temperature is calculated using equation 14:

$$T_r = \frac{(235^\circ F + 460) / 1.8 \ ^\circ K / ^\circ F}{T_c\ (CO_2)} = \frac{386.1^\circ K}{304.2^\circ K} = 1.27$$

Look up values of reduced viscosity at several reduced pressures along a vertical line along Tr = 1.27 in figure 2 using equations 12 and 13.

i.e. at $P_r = 2.0$, $\mu_r = 0.753$

$$\mu = \mu_r \bullet \mu_c (CO_2) = 0.753 \bullet 3335 \bullet 10^{-5}\ \text{cp} = 0.0251\ \text{cp}$$

$$p = P_r \bullet P_c (CO_2) = 2.0 \bullet 72.8\ \text{atm} \bullet 14.696\ \text{PSI / atm} = 2139.7\ \text{PSI}$$

This procedure is repeated for several of pressures between 14.7 PSI and a pressure above the maximum pressure in the pressure transient test. CO_2 compressibility at reservoir temperature and the same pressures can be determined directly from table 4.

Example 2: Enriched Gas Well

Reservoir Temperature: 185°F
Reservoir Pressure: 1875 PSI
Miscible Gas Composition:

Component	Mole %
CH_4	59.13
C_2H_6	7.16
C_3H_8	27.39
C_4H_{10}	3.31
C_5H_{12}	1.60
C_6H_{14}	1.41

First the critical pressure and temperature of the gas mix are calculated with the mixing rules described in equations 15 - 18 and the component critical properties contained in table 5:

$$J = \frac{1}{3}\left(0.5913 \cdot \frac{190.6}{45.4} + 0.0716 \cdot \frac{305.4}{48.2} + 0.2739 \cdot \frac{369.8}{41.9} + 0.0331 \cdot \frac{425.2}{37.5} + 0.0160 \cdot \frac{469.6}{33.3} + 0.0141 \cdot \frac{507.4}{29.3}\right) +$$

$$\frac{2}{3}\left(0.5913\sqrt{\frac{190.6}{45.4}} + 0.0716\sqrt{\frac{305.4}{48.2}} + 0.2739\sqrt{\frac{369.8}{41.9}} + 0.0331\sqrt{\frac{425.2}{37.5}} + 0.0160\sqrt{\frac{469.6}{33.3}} + 0.0141\sqrt{\frac{507.4}{29.3}}\right)^2$$

$$J = \frac{1}{3}\,(6.199) + \frac{2}{3}\,(2.436)^2 = 6.022$$

$$K = \left(0.5913 \cdot \frac{190.6}{\sqrt{45.4}} + 0.0716 \cdot \frac{305.4}{\sqrt{48.2}} + 0.2739 \cdot \frac{369.8}{\sqrt{41.9}} + 0.0331 \cdot \frac{425.2}{\sqrt{37.5}} + 0.016 \cdot \frac{469.6}{\sqrt{33.3}} + 0.0141 \cdot \frac{507.4}{\sqrt{29.3}}\right)$$

$$K = 40.45$$

$$Tc = K^2 / J = 40.45^2 / 6.022 = 271.7^\circ K$$

$$Pc = Tc / J = 271.7 / 6.022 = 45.1 \text{ atm}$$

Next reduced temperature is calculated using equation 14:

$$Tr = \frac{(185^\circ F + 460) / 1.8 \ ^\circ K / ^\circ F}{Tc} = \frac{358.3^\circ K}{271.7^\circ K} = 1.32$$

Look up values of compressibility at several reduced pressures by interpolating between 1.3 and 1.35 reduced temperatures in figures 3 and 4.

i.e. at $P_r = 3.0$ and $T_r = 1.32$; z factor = 0.64

$p = P_r \cdot P_c = 3.0 \cdot 45.1 \text{ atm} \cdot 14.696 \text{ PSI / atm} = 1988.4 \text{ PSI}$

This procedure is repeated for several of pressures between 14.7 PSI and a pressure above the maximum pressure in the pressure transient test.

Gas viscosities at the same pressures that the gas compressibilities were calculated, can be determined from equations 19 - 25 with component critical data from Table 5:

$$M = (0.5913 \cdot 16.043 + 0.0716 \cdot 30.070 + 0.2739 \cdot 44.097 + 0.0331 \cdot 58.124 + 0.0160 \cdot 72.151 + 0.0141 \cdot 86.178)$$

$$= 28.011 \text{ g/mol}$$

$$Vc = (0.5913 \cdot 99.0 + 0.0716 \cdot 148. + 0.2739 \cdot 203. + 0.0331 \cdot 255. + 0.0160 \cdot 304. + 0.0141 \cdot 370.)$$

$$= 143.3 \text{ cm}^3\text{/g-mol}$$

$$\xi = 271.7^{1/6} / 28.011^{1/2}\, 45.1^{2/3} = 0.0380$$

$$\mu^o = (3.40 \cdot 1.27^{8/9}) / 0.0380 = 110.7 \, \mu\text{P}$$

$$V = (0.64 \cdot 82.07 \cdot 386.1^o\text{K}) / 45.1 \text{ atm} = 453.1 \text{ cm}^3\text{/g-mol}$$

$$\rho r = 143.3 \text{ cm}^3\text{/g-mol} / 453.1 \text{ cm}^3\text{/g-mol} = 0.316$$

$$(\mu - 110.7)\, 0.0380 = 1.08 \left[\exp 1.439 \cdot 0.316 - \exp (-1.11 \cdot 0.316^{1.858}) \right]$$

$$\mu = 130.5 \, \mu\text{p} = 0.01305 \text{ cp}$$

Example 3: Enriched Gas Well Contaminated with CO_2

Reservoir Temperature: 200°F
Reservoir Pressure: 3375 PSI
Miscible Gas Composition:

Component	Mole %
CO_2	22.51
CH_4	23.61
C_2H_6	22.58
C_3H_8	27.92

C_4H_{10}	1.76
iso-C_4H_{10}	1.62

As in example 2, the critical pressure and temperature of the gas mix are calculated with the mixing rules described in equations 15 - 18 and the component critical properties contained in table 5:

$$J = \frac{1}{3}\left(0.2251 \cdot \frac{304.2}{72.8} + 0.2361 \cdot \frac{190.6}{45.4} + 0.2258 \cdot \frac{305.4}{48.2} + 0.2792 \cdot \frac{369.8}{41.9} + 0.0176 \cdot \frac{425.2}{37.5} + 0.0162 \cdot \frac{408.1}{36.0}\right) +$$

$$\frac{2}{3}\left(0.2251\sqrt{\frac{304.2}{72.8}} + 0.2361\sqrt{\frac{190.6}{45.4}} + 0.2258\sqrt{\frac{305.4}{48.2}} + 0.2792\sqrt{\frac{369.8}{41.9}} + 0.0176\sqrt{\frac{425.2}{37.5}} + 0.0162\sqrt{\frac{408.1}{36.0}}\right)^2$$

$$J = \frac{1}{3}(6.210) + \frac{2}{3}(2.456)^2 = 6.091$$

$$K = \left(0.2251 \cdot \frac{304.2}{\sqrt{72.8}} + 0.2361 \cdot \frac{190.6}{\sqrt{45.4}} + 0.2258 \cdot \frac{305.4}{\sqrt{48.2}} + 0.2792 \cdot \frac{369.8}{\sqrt{41.9}} + 0.0176 \cdot \frac{425.2}{\sqrt{37.5}} + 0.0162 \cdot \frac{408.1}{\sqrt{36.0}}\right)$$

$K = 42.91$

$Tc = K^2 / J = 42.91^2 / 6.091 = 302.3^oK$

$Pc = Tc / J = 302.3 / 6.091 = 49.6$ atm

Employing equations 26 - 28 to correct for the presence of CO_2:

$\varepsilon = 120 \cdot (0.2251^{0.9} - 0.2251^{1.6}) = 20.3$

$Tc = 302.3^oK - 20.3^oK = 282.0^oK$

$$Pc = \frac{49.6 \text{ atm} \cdot 282.0^oK}{302.3^oK} = 46.3 \text{ atm}$$

Next reduced temperature is calculated using equation 14:

$$Tr = \frac{(200^oF + 460) / 1.8 \ ^oK / ^oF}{Tc} = \frac{366.7^oK}{282.0^oK} = 1.30$$

Look up values of compressibility at several reduced pressures at 1.30 reduced temperature in figures 3 and 4.

i.e. at $P_r = 3.0$ and $T_r = 1.30$; z factor = 0.62

$$p = P_r \cdot P_c = 3.0 \cdot 46.3 \text{ atm} \cdot 14.696 \text{ PSI / atm} = 2041.3 \text{ PSI}$$

This procedure is repeated for several of pressures between 14.7 PSI and a pressure above the maximum pressure in the pressure transient test.

Gas viscosities at the same pressures that the gas compressibilities were calculated at, can be determined from equations 19 - 25 with component critical data from Table 5:

$$M = (0.2251 \cdot 44.010 + 0.2361 \cdot 16.043 + 0.2258 \cdot 30.070 + 0.2792 \cdot 44.097 + 0.0176 \cdot 58.124 + 0.0162 \cdot 58.124)$$
$$= 34.761 \text{ g/mol}$$

$$Vc = (0.2251 \cdot 94.0 + 0.2361 \cdot 99.0 + 0.2258 \cdot 148. + 0.2792 \cdot 203. + 0.0176 \cdot 255. + 0.0162 \cdot 263.)$$
$$= 143.4 \text{ cm}^3\text{/g-mol}$$

$$\xi = 282.0^{1/6} / 34.761^{1/2} \, 46.3^{2/3} = 0.0337$$

$$\mu^o = (3.40 \cdot 1.30^{8/9}) / 0.0337 = 127.4 \, \mu P$$

$$V = (0.62 \cdot 82.07 \cdot 366.7^oK) / 45.1 \text{ atm} = 453.1 \text{ cm}^3\text{/g-mol}$$

$$\rho r = 143.3 \text{ cm}^3\text{/g-mol} / 453.1 \text{ cm}^3\text{/g-mol} = 0.316$$

$$(\mu - 110.7) \, 0.0380 = 1.08 \left[\exp 1.439 \cdot 0.316 - \exp(-1.11 \cdot 0.316^{1.858}) \right]$$

$$\mu = 130.5 \, \mu p = 0.01305 \text{ cp}$$

CONCLUSIONS

1) The real gas pseudo-pressure approach to pressure transient analysis of gas wells is applied to wells injecting or producing predominatly miscible gas (either CO_2 or enriched natural gas).

2) The method was used to analyze injection and production well pressure transient tests in two CO_2 field projects; and example calculations illustrate this approach for two additional cases: an enriched gas well and an enriched gas well contaminated with CO_2 / H_2S.

3) In addition to flow capacity, fracturing, and wellbore damage or stimulation (skin factor); wellbore volume, reservoir pressure, reserves, reservoir discontinuities, fluid discontinuities, and swept volume may be determined using the real gas pseudo-pressure if the appropriate data is available.

SYMBOLS

A = mole fraction (CO_2 + H_2S)
B = mole fraction H_2S
B_g = formation volume factor for gas
C_i = spline fit constant for ith data pair
C_g = gas compressibility
C_t = total compressibility
q_j = injection rate, MCF/D
$J = 1/3 \sum y_j \bullet (T_c/P_c)_i + (2/3) \bullet [\sum y_j \bullet (T_c/P_c)_i^{0.5}]^2$
$K = \sum y_j \bullet (T_c/P_c)_i^{0.5}$
k = permeability, md
k_g = effective gas permeability, md
k_{rg} = relative permeability to gas
M = average molecular weight, g/mole
M_j = molecular weight of component j, g/mole
$m(p)$ = real gas pseudo-pressure
n = number of injection rates
p = pressure, PSI or atm
p_b = base pressure, PSI or atm
P_c = critical pressure, PSI or atm
p_i = initial shut in pressure, PSI or atm
P_r = reduced pressure

p_{1hr} = extrapolated pressure at 1 hr shut in time, PSI or atm
q = flow rate, MCF/D
R = gas constant, (cm^3 atm)/(g-mole °K)
r = radial distance, ft
r_w = wellbore radius, ft
T = temperature, °K, °C, or °F
t_j = absolute time to the end of the jth rate, hr
t_n = absolute time to the end of the last rate, hr
t_s = shut in time, hr
V = volume, cm^3/g-mole
V_c = critical volume, cm^3/g-mole
V_{cj} = critical volume of component j, cm^3/g-mole
X_{int} = interpolated x value
y_j = mole fraction of component i
Y_{int} = interpolated y value
z = compressibility factor
$\varepsilon = 120 (A^{0.9} - A^{1.6}) + 15 (B^{0.5} - B^4)$
ϕ = porosity
μ = viscosity, cp
μ_c = critical viscosity, cp
μ^o = low pressure viscosity, cp
μ_r = reduced viscosity
ρ_r = reduced density
$\xi = Tc^{1/6} / M^{1/2} Pc^{2/3}$

REFERENCES

1. Earlougher, R.C. Jr.: Advances In Well Test Analysis, Monograph Series, SPE, Dallas (1977) **5**.

2. "Pressure Transient Analysis Reservoir Engineering", ARCO Oil and Gas Company Training Manual (1982).

3. Satman, A., Eggenschwiler, M., and Ramey, H.J.Jr., "Interpretation of Injection Well Pressure Transient Data in Thermal Oil Recovery", SPE 8908, California Regional Meeting, Los Angeles (1980).

4. Messner, G.L., and Williams, R.L., "Application of Pressure Transient Analysis in Steam Injection Wells", SPE 10781, California Regional Meeting, San Francisco (1982).

5. Al-Hussainy, R. Ramey, H.J.Jr., and Crawford, P.B.,"The Flow of Real Gasses Through Porous Media", J. Pet. Tech., (May,1966).

6. Sage, B.H. and Lacy, W.N.: Some Properties of the Lighter Hydrocarbons, Hydrogen Sulfide, and Carbon Dioxide, American Petroleum Institute (1955).

7. Kennedy, J.T., and Thodos, G., "The Transport Properties of Carbon Dioxide", AIChE J., (Dec, 1961).

8. Sutton, R.P., "Compressibility Factors for High-Molecular-Weight Reservoir Gasses", SPE 14265, 60th Annual Meeting, Las Vegas (1985).

9. Stewart, W.F., Burkhardt, S.F., and Voo D., "Prediction of Pseudocritical Parameters for Mixtures", paper presented at the AICHE Meeting, Kansas City (1959).

10. Dranchuk, P.M. and Abou-Kassem, J.H., "Calculation of Z Factors for Natural Gasses Using Equations of State", J. Cdn. Pet. Tech., (July-Sept, 1975).

11. Dean, D.E., and Stiel, L.I., AIChE J., **11**(1965).

12. Wichert, E., and Aziz, K., "Calculate Z's for Sour Gases", Hyd. Proc., (May,1972).

13. Johnson, L.W. and Reiss, R.D.: Numerical Analysis, Addison-Wesley Pub. Co. (1977).

14. Reid, R.C., Prausnitz J.M., and Sherwood, T.K.: The Properties of Gases and Liquids, McGraw-Hill Book Company, 3rd Edition (1977).

Table 1
Pressure Transient Analysis Results

WELL #	SLOPE PSI**2/cp*cycle	kk_rh md*ft	$m(P1_{hr})$ PSI**2/cp	m(Pi) PSI**2/cp	SKIN	FRACTURE EVIDENCE
RESERVOIR 1						
CO_2 INJECTION WELLS						
18	n/a	n/a	n/a	57.21×10^7	n/a	no*
29	1.61×10^6	1949	46.57×10^7	47.07×10^7	-1.8	no
29, 1983	2.26×10^6	1046	40.99×10^7	41.01×10^7	-5.0	no
39	3.75×10^6	1315	47.36×10^7	48.94×10^7	-0.2	no
52	2.33×10^6	1490	39.83×10^7	40.43×10^7	-2.0	no
64	n/a	n/a	n/a	40.74×10^7	n/a	yes
74	n/a	n/a	n/a	45.24×10^7	n/a	yes
74, 1983	1.78×10^7	102	44.10×10^7	47.15×10^7	-2.0	no
87	2.00×10^6	3137	30.20×10^7	39.37×10^7	47	no
PRODUCTION WELLS						
84	7.30×10^7	14.6	26.50×10^7	19.44×10^7	-2.2	no
95	1.35×10^7	94.0	17.80×10^7	15.67×10^7	-2.3	no
409	2.60×10^7	28.4	56.24×10^7	52.01×10^7	-2.2	no**
RESERVOIR 2						
CO_2 INJECTION WELLS						
62-32	n/a	n/a	n/a	n/a	n/a	yes
487-29	8.0×10^6	140	92.24×10^7	94.16×10^7	-1.9	no
488-29	n/a	n/a	n/a	n/a	n/a	yes

* data invalid, storage dominated

** data questionable due to pressure leak

Table 2
Well Summary

WELL #	SHUT-IN FLOW RATE, MCF/D	TEMP °F	THICKNESS ft.	POROSITY FRACTION	WELLBORE RADIUS, ft.	C_t PSI^{-1}
RESERVOIR 1						
CO_2 INJECTION WELLS						
18	1170	117	140	0.165	0.292	$30.96x10^{-6}$
29	3340	114	121	0.18	0.292	$37.98x10^{-6}$
39	6167	114	133	0.205	0.292	$37.38x10^{-6}$
52	6211	109	165	0.212	0.292	$45.29x10^{-6}$
64	2670	110	176	0.211	0.292	$42.65x10^{-6}$
74	3326	107	140	0.203	0.292	$35.99x10^{-6}$
87	6760	99	37	0.210	0.292	$44.3\ x10^{-6}$
PRODUCTION WELLS						
84	1139	110	172	0.185	0.292	$105.0\ x10^{-6}$
95	1365	108	248	0.160	0.292	$97.2\ x10^{-6}$
409	777	120	141	0.159	0.292	$31.9\ x10^{-6}$
RESERVOIR 2						
CO_2 INJECTION WELLS						
62-32	813	235	126	0.18	0.292	$1.09x10^{-4}$
487-29	985	235	143	0.15	0.292	$1.09x10^{-4}$
488-29	1330	235	149	0.15	0.292	$1.09x10^{-4}$

Table 3
CO_2 Properties

	Tr=1.02		Tr=1.03		Tr=1.04		Tr=1.05	
	T=99°F		T=107-108°F		T=109-110°F		T=114-120°F	
PRESSURE PSI	μ cp	z	μ cp	z	μ cp	z	μ cp	z
4266.9							0.0867	0.5465
3196.5	0.0834	0.4311	0.0800	0.4383	0.0777	0.4403	0.0740	0.4455
2126.1	0.0704	0.3266	0.0644	0.3395	0.0610	0.3432	0.0550	0.3530
1590.9	0.0550	0.2821	0.0477	0.3082	0.0407	0.3164	0.0351	0.3403
1055.7	0.0205	0.5249	0.0203	0.5702	0.0202	0.5797	0.0200	0.6013
841.6	0.0183	0.6610	0.0183	0.6839	0.0183	0.6892	0.0183	0.7017
627.5	0.0168	0.7640	0.0169	0.7773	0.0171	0.7805	0.0172	0.7881
413.5	0.0158	0.8521	0.0160	0.8595	0.0164	0.8613	0.0167	0.8656
199.4	0.0155	0.9315	0.0159	0.9346	0.0159	0.9354	0.0162	0.9373
14.7	0.0152	0.9951	0.0155	0.9953	0.0156	0.9954	0.0158	0.9955

	Tr=1.27	
	T=235°F	
PRESSURE PSI	μ cp	z
5337.3	0.0437	0.7430
4266.9	0.0378	0.6891
3196.5	0.0315	0.6629
2126.1	0.0251	0.7045
1590.9	0.0233	0.7607
1055.7	0.0212	0.8339
627.5	0.0207	0.8993
14.7	0.0201	0.9976

Table 4
Volumetric Properties of CO_2

	40 F		100F		160 F		220 F	
	Compressibility Factor	Volume (CuFt Per lb. Mole)	Compressibility Factor	Volume (CuFt Per lb. Mole)	Compressibility Factor	Volume (CuFt Per lb. Mole)	Compressibility Factor	Volume (CuFt Per lb. Mole)
	(566.5)[a]							
DP	0.6619	6.287						
BP	0.08247	0.7807						
200	0.9057	24.28	0.9375	28.16	0.9562	31.8	0.9685	35.3
400	0.7936	10.64	0.8692	13.05	0.9107	15.14	0.9366	17.08
600	0.08720	0.7794	0.7926	7.93	0.8630	9.57	0.9042	10.99
800	0.1153	0.7728	0.7028	5.28	0.8127	6.76	0.8716	7.95
1,000	0.1429	0.7662	0.5868	3.52	0.7591	5.05	0.8387	6.12
1,250	0.1768	0.7587	0.2970	1.427	0.6876	3.66	0.7974	4.65
1,500	0.2103	0.7517	0.2560	0.025	0.6125	2.715	0.7566	3.68
1,750	0.2429	0.7442	0.2768	0.9501	0.5398	2.051	0.7171	2.989
2,000	0.2748	0.7367	0.3019	0.9066	0.4850	1.613	0.6814	2.485
2,250	0.3063	0.7301	0.3284	0.7867	0.4590	1.357	0.6510	2.110
2,500	0.3373	0.7235	0.3555	0.8542	0.4554	1.211	0.6280	1.832
2,750	0.3676	0.7169	0.3828	0.8362	0.4632	1.120	0.6134	1.627
3,000	0.3976	0.7108	0.4102	0.8212	0.4772	1.058	0.6060	1.473
3,500	0.4558	0.6984	0.4644	0.7970	0.5132	0.9751	0.6113	1.274
4,000	0.5125	0.6871	0.5185	0.7785	0.5567	0.9255	0.6323	1.153
4,500	0.5680	0.6769	0.5714	0.7627	0.6015	0.8890	0.6611	1.072
5,000	0.6235	0.6688	0.6239	0.7495	0.6472	0.8608	0.6951	1.014
6,000	0.7342	0.6562	0.7263	0.7270	0.7385	0.8186	0.7700	0.9361
7,000	0.8439	0.6465	0.8282	0.7107	0.8292	0.7878	0.8481	0.8837
8,000	0.9507	0.6373	0.9280	0.6968	0.9185	0.7636	0.9282	0.8463
9,000	1.0562	0.6293	1.0254	0.6844	1.0065	0.7438	1.0078	0.8168
10,000	1.1604	0.6223	1.1203	0.6729	1.0946	0.7279	0.0872	0.7931

	280 F		340 F		400 F		400 F	
200	0.9771	38.8	0.9834	42.2	0.9880	45.6	0.9916	48.9
400	0.9543	18.94	0.9670	20.75	0.9762	22.52	0.9834	24.27
600	0.9317	12.33	0.9509	13.60	0.9647	14.83	0.9755	16.05
800	0.9092	9.02	0.9352	10.03	0.9535	11.00	0.9678	11.94
1,000	0.8870	7.04	0.9200	7.90	0.9427	8.70	0.9604	9.48
1,250	0.8600	5.46	0.9015	6.19	0.9298	6.86	0.9518	7.52
1,500	0.8338	4.41	0.8841	5.06	0.9179	5.64	0.9438	6.21
1,750	0.8094	3.67	0.8679	4.26	0.9068	4.78	0.9366	5.28
2,000	0.7868	3.12	0.8529	3.66	0.8970	4.14	0.9304	4.59
2,250	0.7669	2.706	0.8397	3.20	0.8884	3.64	0.9249	4.06
2,500	0.7500	2.381	0.8282	2.842	0.8811	3.25	0.9205	3.63
2,750	0.7365	2.126	0.8192	2.557	0.8754	2.937	0.9171	3.29
3,000	0.7264	1.922	0.8120	2.323	0.8709	2.678	0.9146	3.01
3,500	0.7185	1.630	0.8045	1.973	0.8663	2.283	0.9123	2.573
4,000	0.7234	1.436	0.8049	1.727	0.8660	1.997	0.9134	2.254
4,500	0.7380	1.302	0.8117	1.548	0.8710	1.786	0.9177	2.013
5,000	0.7601	1.207	0.8248	1.416	0.8810	1.626	0.9259	1.828
6,000	0.8156	1.079	0.8660	1.239	0.9126	1.403	0.9526	1.567
7,000	0.8802	0.9987	0.9180	1.125	0.9553	1.259	0.9880	1.393
8,000	0.9483	0.9409	0.9750	1.046	1.0036	1.157	1.0303	1.271
9,000	1.0489	0.8987	1.0365	0.9884	1.0570	1.084	1.0777	1.182
10,000	1.0900	0.8652	1.1015	0.9453	1.1148	1.029	1.1272	1.113

---

[a] Two-Phase Pressure, in psia

Table 5
Component Critical Properties[14]

FORMULA	MOLE WT g/mole	CRITICAL PRESS. atm	CRITICAL TEMP. °K	CRITICAL VOL. cm³/g-mol
CO_2	44.010	72.8	304.2	94.0
H_2S	34.080	88.2	373.2	98.5
N_2	28.013	33.5	126.2	89.5
CH_4	16.043	45.4	190.6	99.0
C_2H_6	30.070	48.2	305.4	148.
C_3H_8	44.097	41.9	369.8	203.
C_4H_{10}	58.124	37.5	425.2	255.
iso-C_4H_{10}	58.124	36.0	408.1	263.
C_5H_{12}	72.151	33.3	469.6	304.
iso-C_5H_{12}	72.151	33.4	460.4	306.
C_6H_{14}	86.178	29.3	507.4	370.

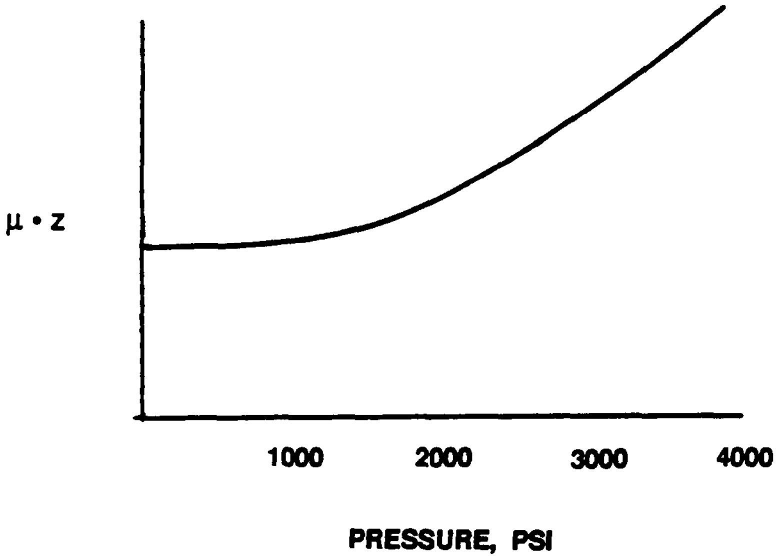

NOTE: **$\mu \cdot z$ is constant below 2000 PSI.**

$\frac{\mu \cdot z}{p}$ is constant above 2000 PSI.

Figure 1—$\mu \bullet z$ vs pressure[2]

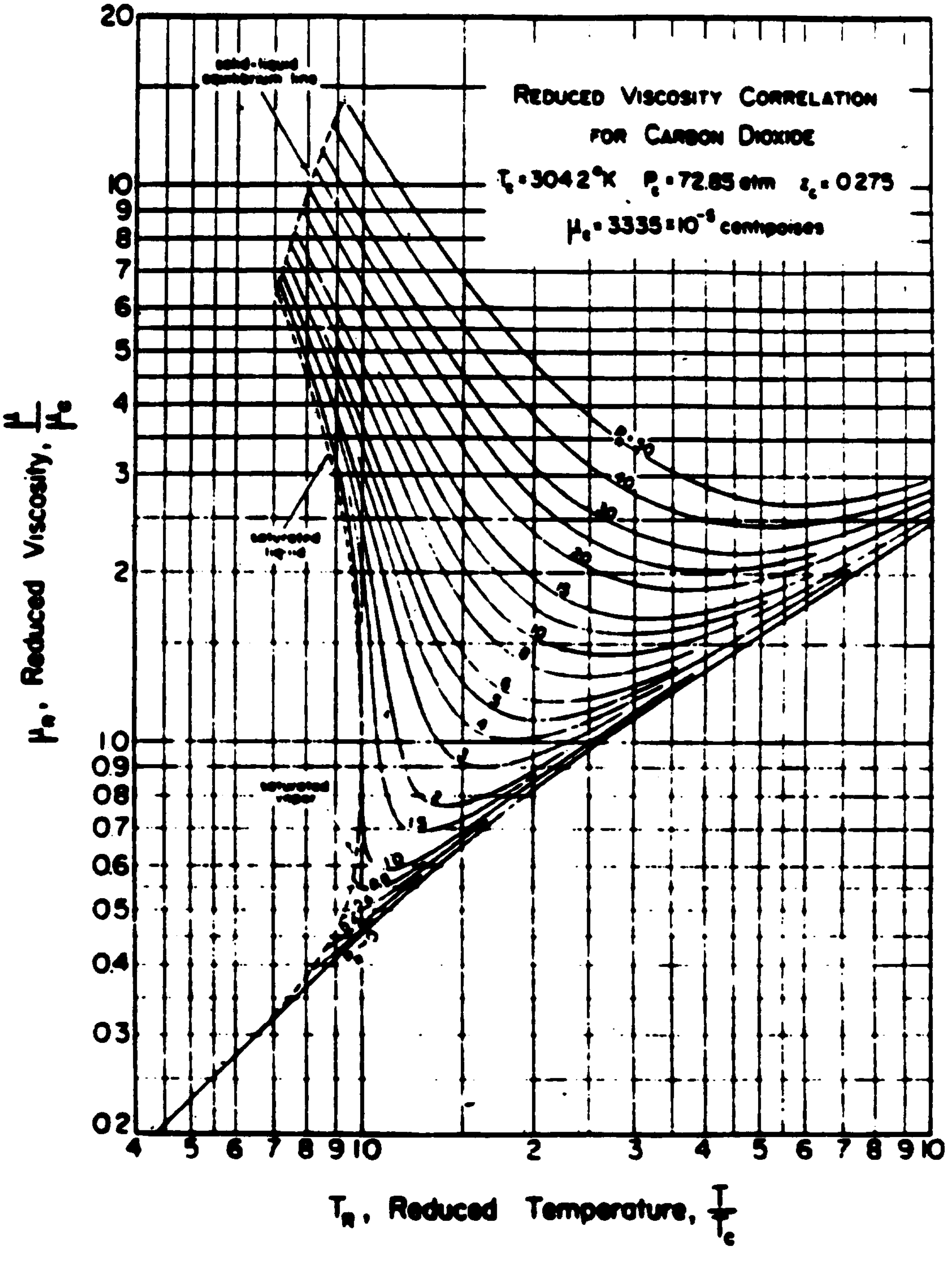

Figure 2—Reduced viscosity correlation for carbon dioxide

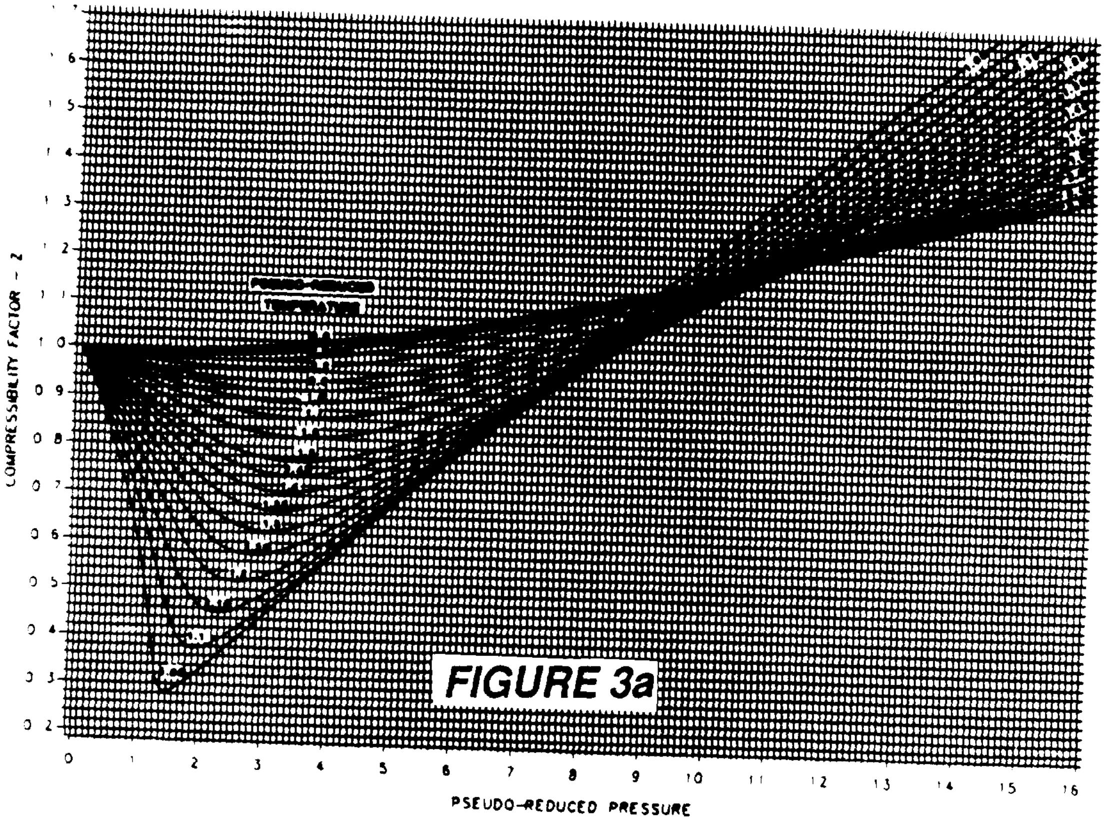

FIGURE 3a

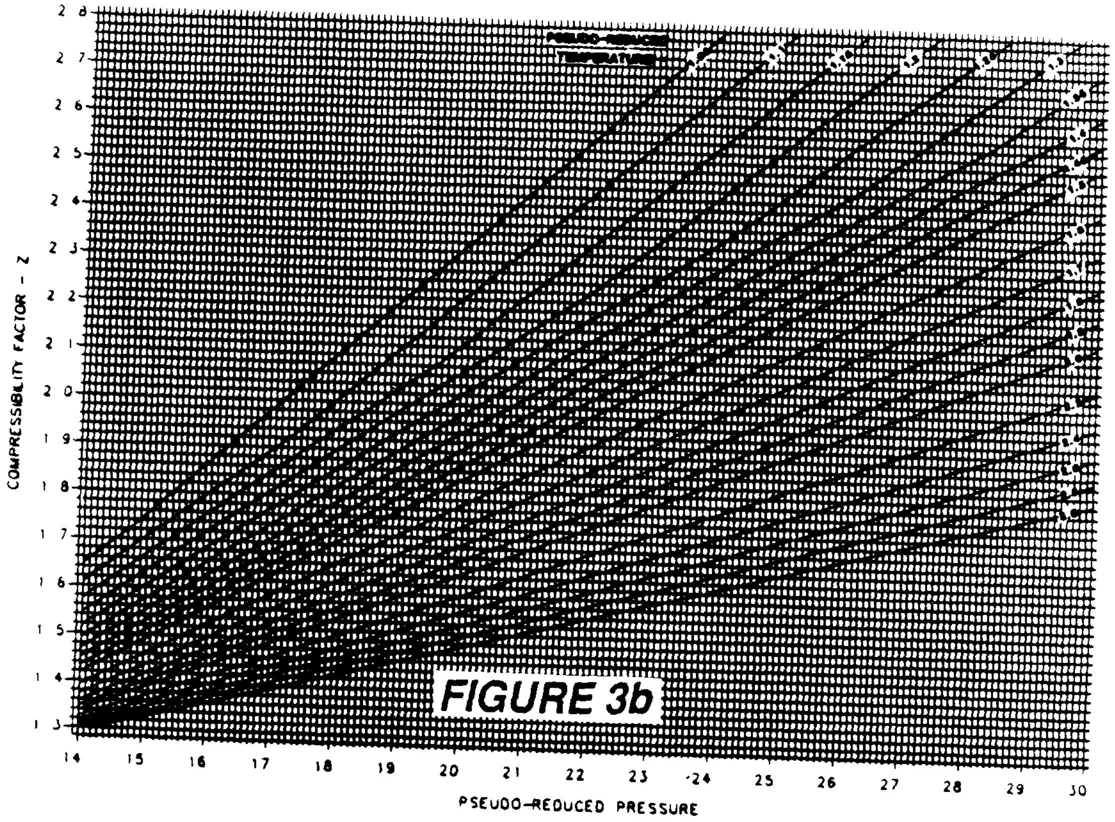

FIGURE 3b

Figures 3a and 3b—Extended gas compressibility factor chart[10]

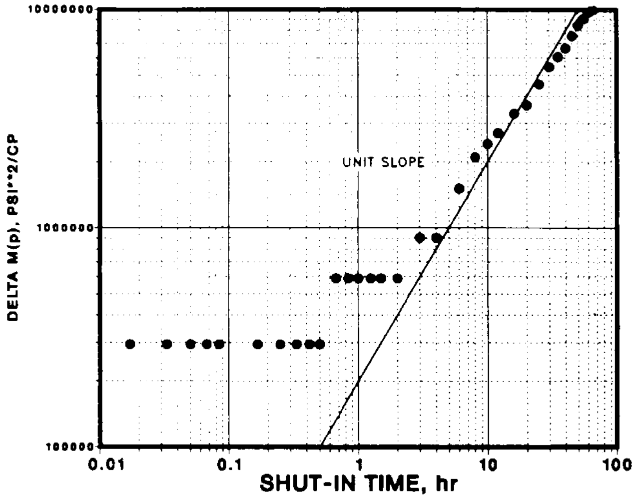

Figure 4—Storage determination
(Reservoir 1 #18)

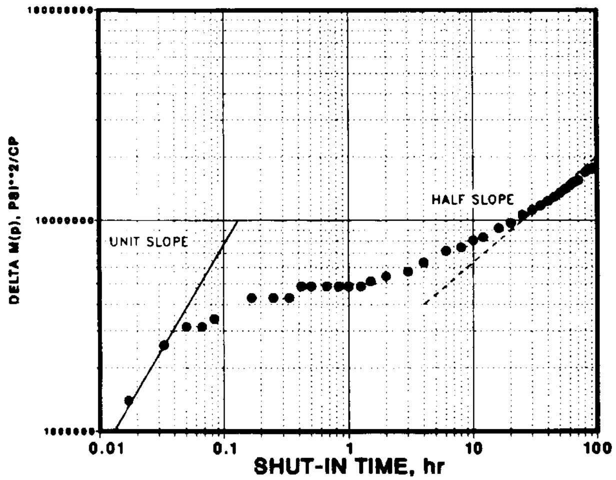

Figure 5—Storage determination
(Reservoir 1 #29)

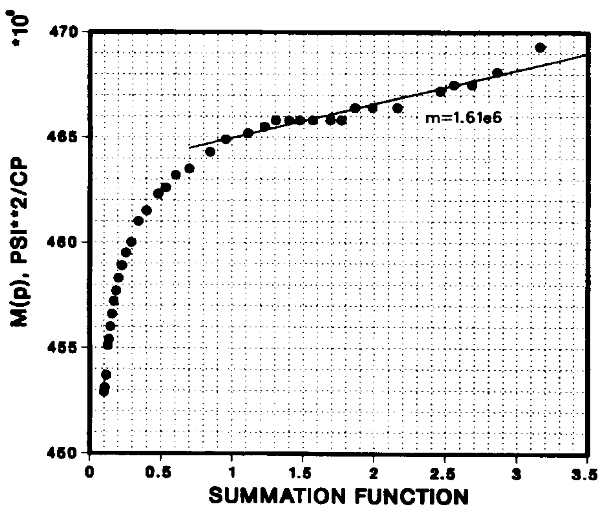

Figure 6—Falloff plot
(Reservoir 1 #29)

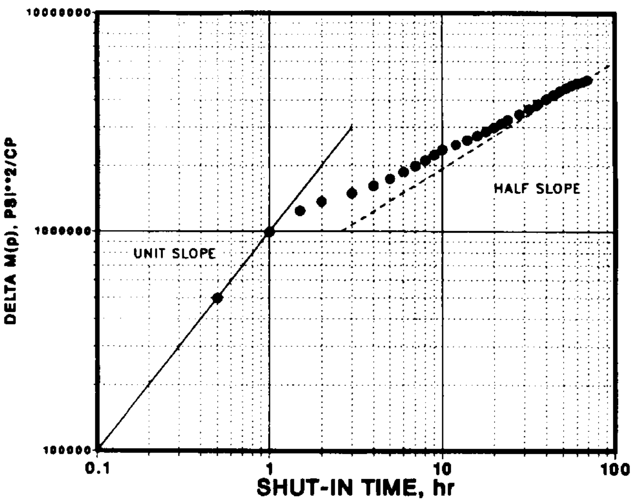

Figure 7—Storage determination
(Reservoir 1 #29-1983)

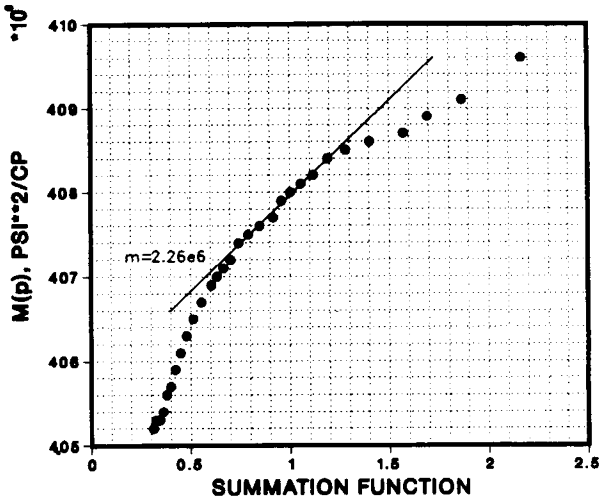

Figure 8—Falloff plot
(Reservoir 1 #29-1983)

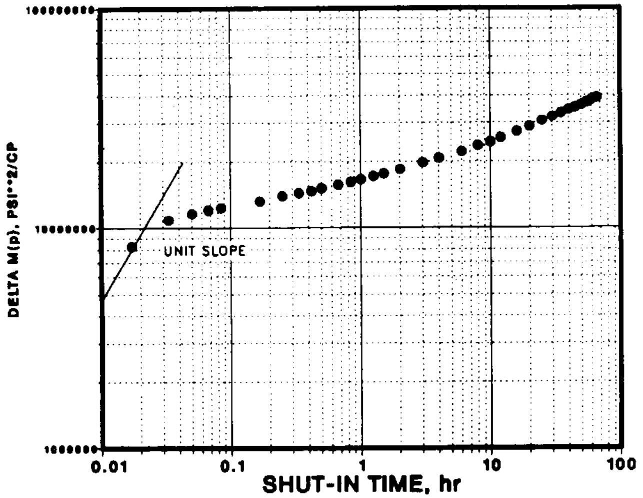

Figure 9—Storage determination
(Reservoir 1 #39)

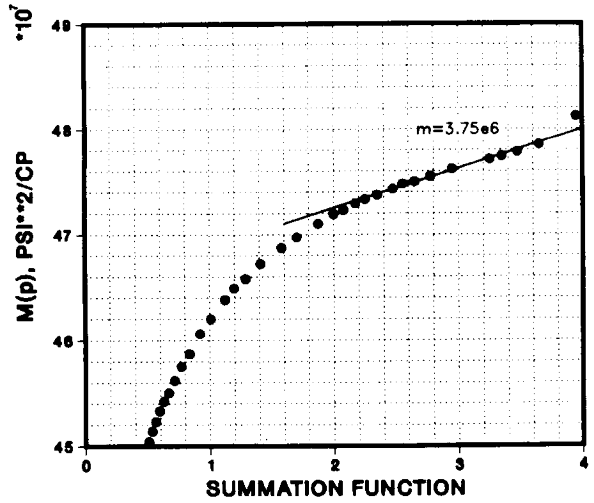

Figure 10—Falloff plot
(Reservoir 1 #39)

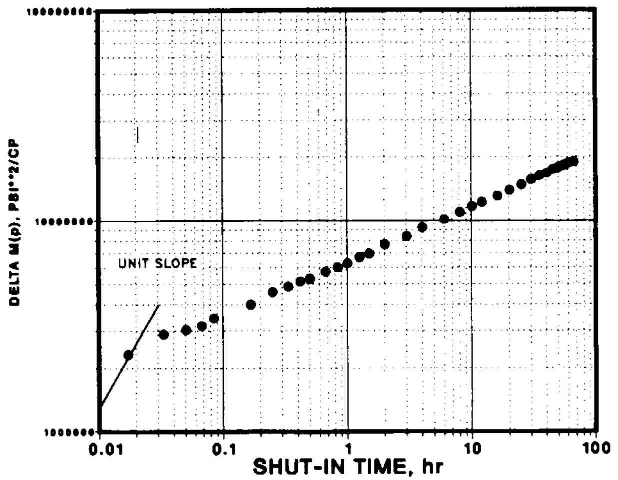

Figure 11—Storage determination
(Reservoir 1 #52)

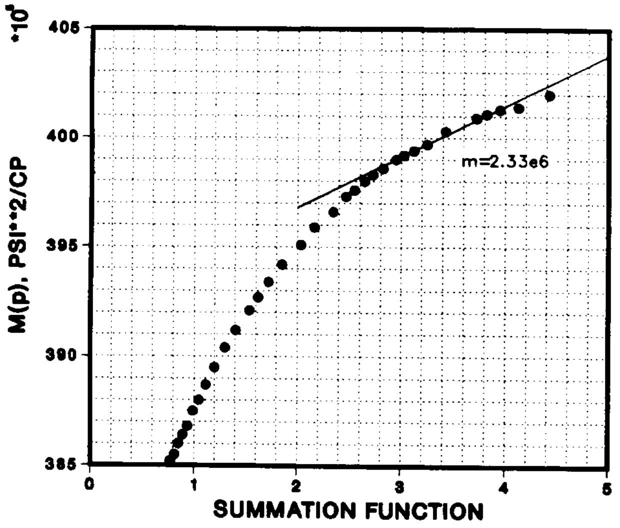

Figure 12—Falloff plot
(Reservoir 1 #52)

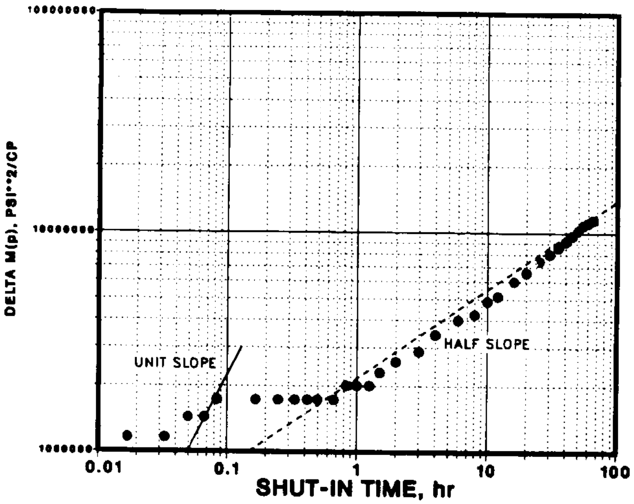

Figure 13—Storage determination
(Reservoir 1 #64)

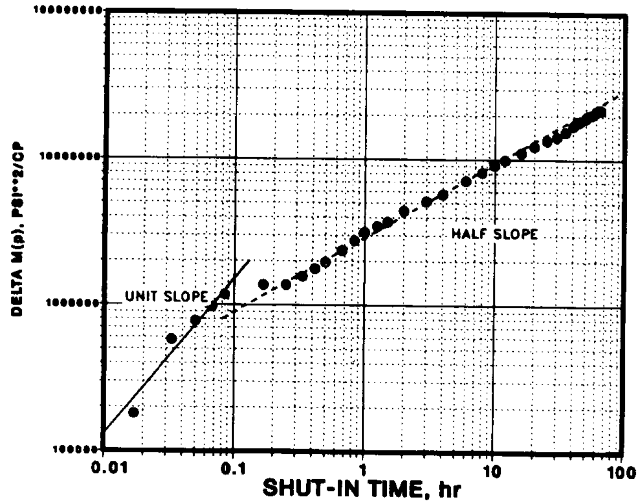

Figure 14—Storage determination
(Reservoir 1 #74)

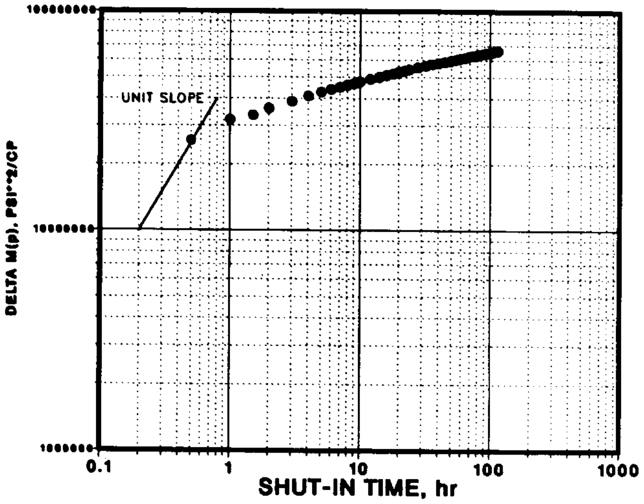

Figure 15—Storage determination
(Reservoir 1 #74-1983)

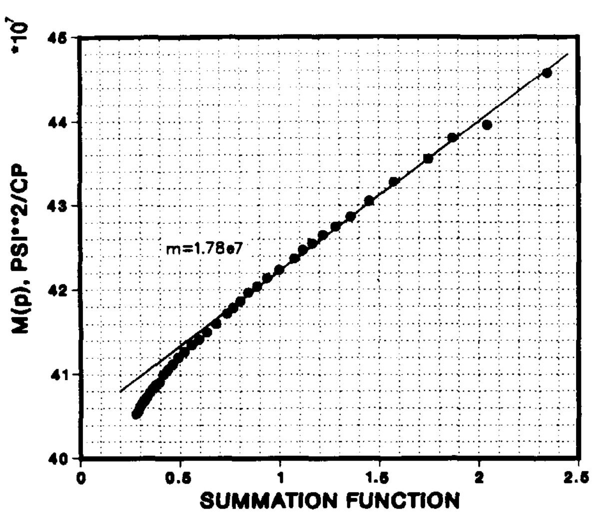

Figure 16—Falloff plot
(Reservoir 1 #74-1983)

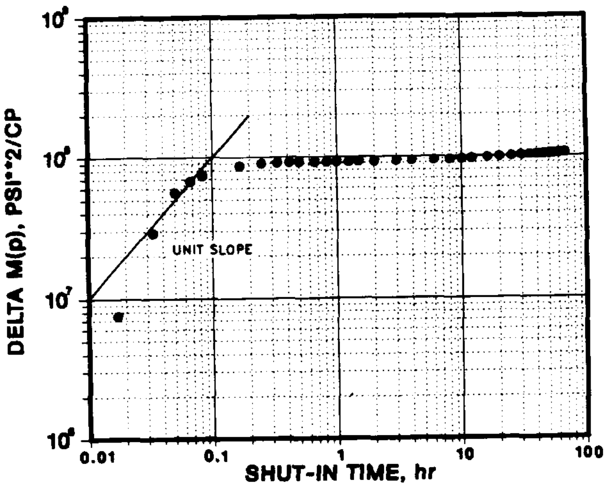

Figure 17—Storage determination
(Reservoir 1 #87)

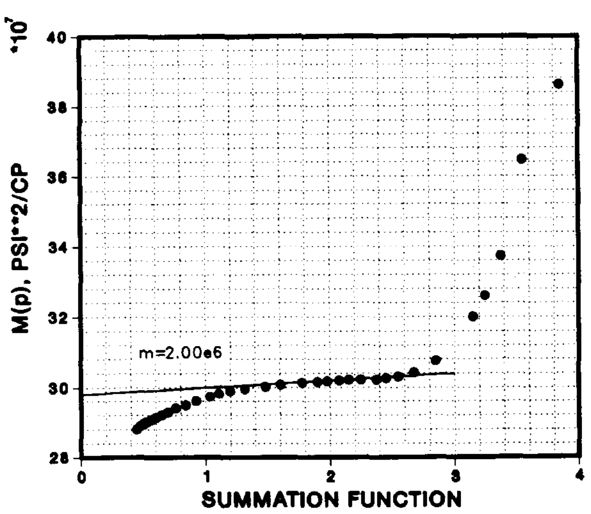

Figure 18—Falloff plot
(Reservoir 1 #87)

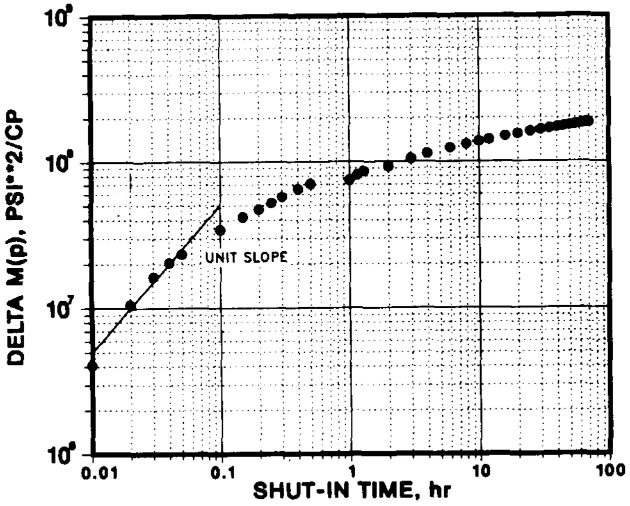

Figure 19—Storage determination
(Reservoir 1 #84)

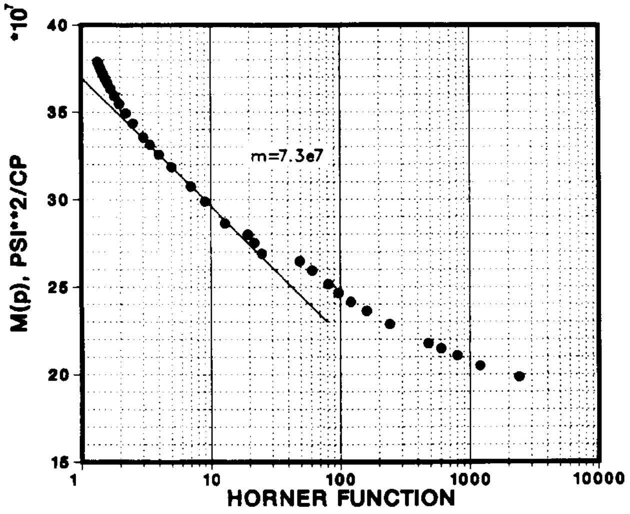

Figure 20—Build-up plot
(Reservoir 1 #84)

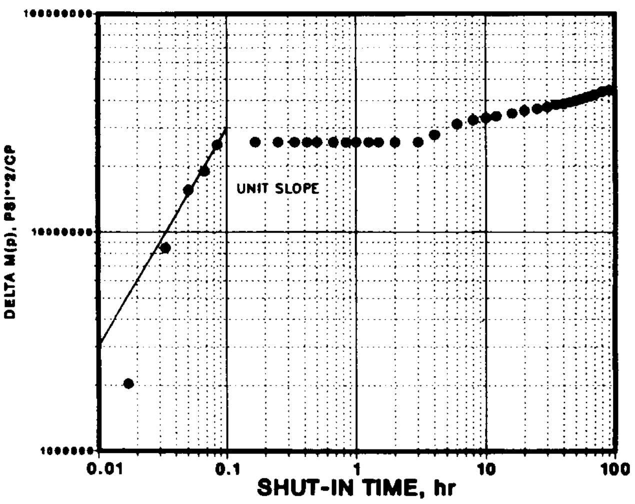

Figure 21—Storage determination
(Reservoir 1 #95)

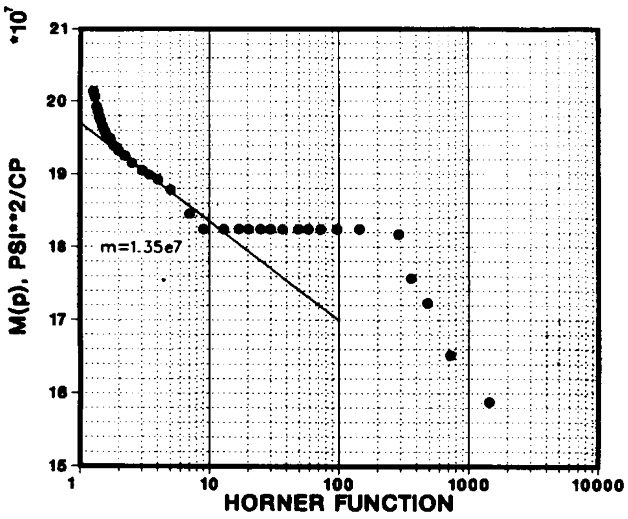

Figure 22—Build-up plot
(Reservoir 1 #95)

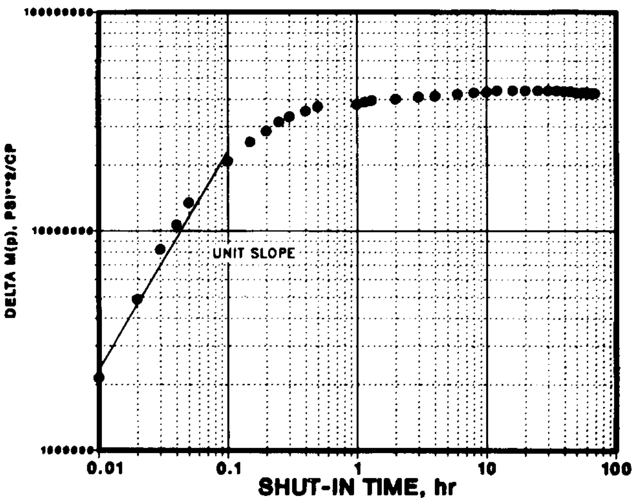

Figure 23—Storage determination
(Reservoir 1 #409)

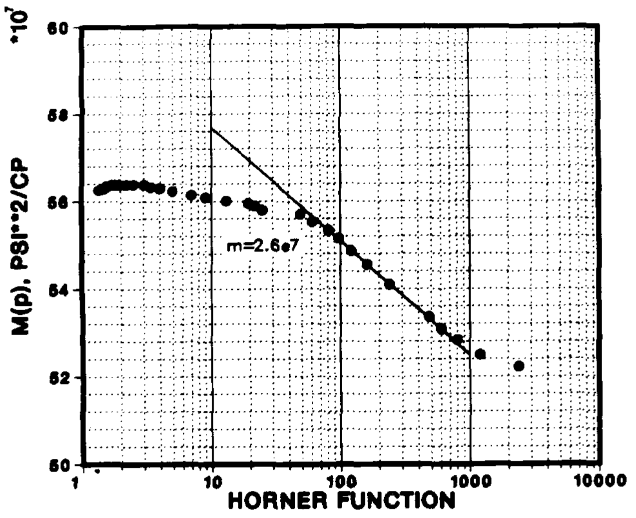

Figure 24—Build-up plot
(Reservoir 1 #409)

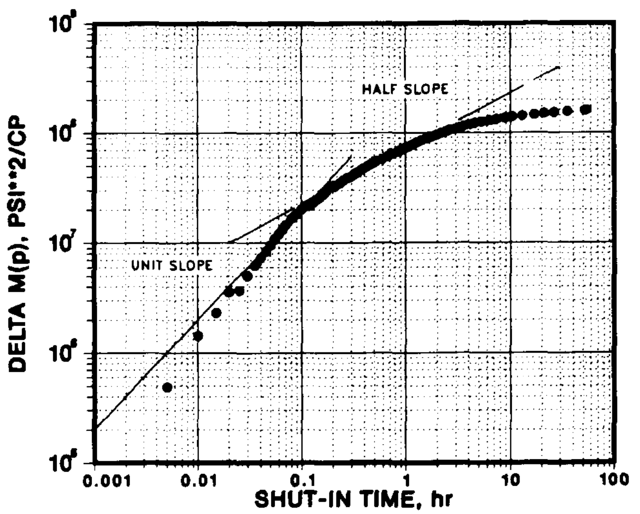

Figure 25—Storage determination
(Reservoir 2 #62)

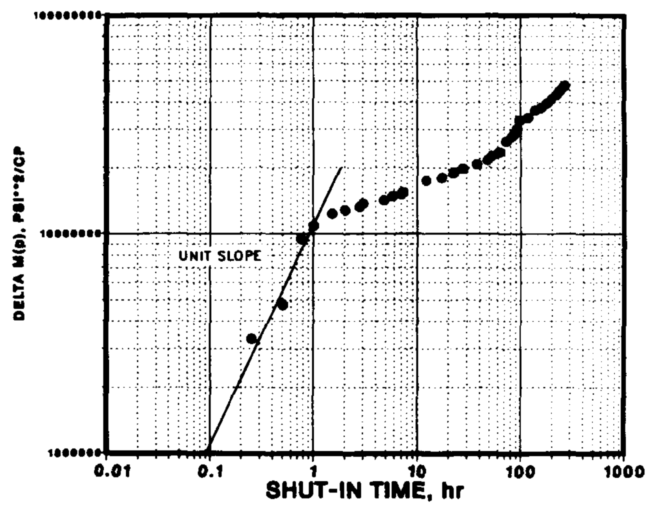

Figure 26—Storage determination
(Reservoir 2 #487)

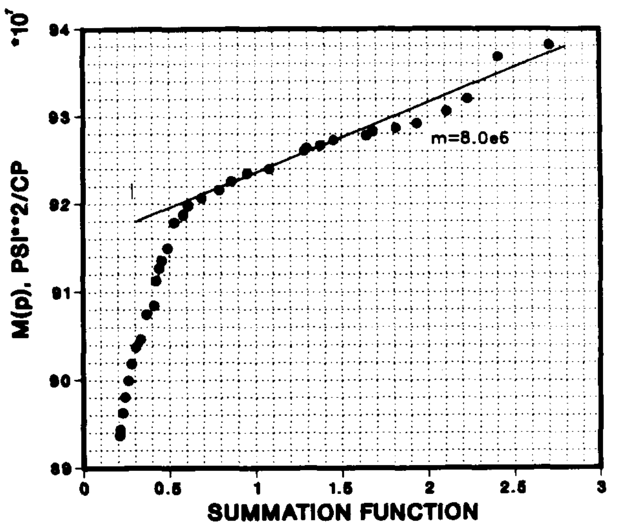

Figure 27—Falloff plot
(Reservoir 2 #487)

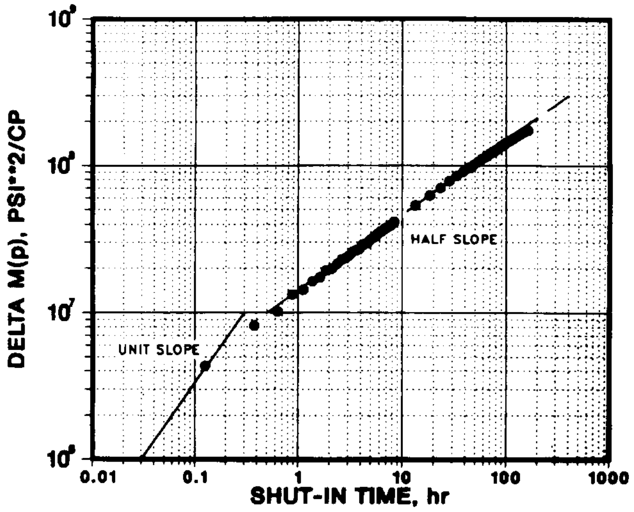

Figure 28—Storage determination
(Reservoir 2 #488)